Are morphological characteristics of Parrotia (Hamamelidaceae) pollen species diagnostic?

Benjamin Adroit, Friðgeir Grímsson, Jean-Pierre Suc, Gilles Escarguel, Reinhard Zetter, Johannes M Bouchal, Séverine Fauquette, Xin Zhuang, Morteza Djamali

Review of Palaeobotany and Palynology 307 (2022) 104776

Contents lists available at ScienceDirect

Review of Palaeobotany and Palynology

journal homepage: www.elsevier.com/locate/revpalbo

Are morphological characteristics of *Parrotia* (Hamamelidaceae) pollen species diagnostic?☆

Benjamin Adroit [a,*], Friðgeir Grímsson [b], Jean-Pierre Suc [c], Gilles Escarguel [d], Reinhard Zetter [e], Johannes M. Bouchal [b], Séverine Fauquette [f], Xin Zhuang [g], Morteza Djamali [h]

[a] Swedish Museum of Natural History, Department of Palaeobiology, Box 50007, 10405 Stockholm, Sweden
[b] University of Vienna, Department of Botany and Biodiversity Research, 1030 Vienna, Austria
[c] Sorbonne Université, CNRS-INSU, Institut des Sciences de la Terre Paris, ISTeP UMR7193, 75005 Paris, France
[d] Laboratoire d'Ecologie des Hydrosystèmes Naturels et Anthropisés UMR CNRS 5023 LEHNA, Université Claude Bernard Lyon 1, France
[e] University of Vienna, Department of Palaeontology, 1090 Vienna, Austria
[f] ISEM, Univ Montpellier, CNRS, EPHE, IRD, Montpellier, France
[g] Institute for Atmospheric and Earth System Research (INAR), University of Helsinki, Finland
[h] Institut Méditerranéen de Biodiversité et d'Ecologie–IMBE (Aix Marseille Univ, Avignon Université, CNRS, IRD), Europôle de l'Arbois, Aix-en-Provence, France

ARTICLE INFO

Article history:
Received 24 August 2022
Received in revised form 20 September 2022
Accepted 22 September 2022
Available online 29 September 2022

Keywords:
Pollen morphology
Tertiary
Relict plant species
Refugia
Hyrcanian forest
Eastern China forest

ABSTRACT

Parrotia persica is one of the most notable endemic relict tree species growing in the Hyrcanian forest at the southern Caspian Sea. The recent discovery of sibling species *Parrotia subaequalis*, occurring in the temperate forests of south-eastern China, offers the opportunity to compare their morphology and ecological preferences and to dig deeper into the paleophytogeographic history of the genus from a perspective. Since pollen morphology of these species would be essential to unravel the origin and evolution of these Arcto-Tertiary species, the present study aimed to investigate whether it is possible to segregate pollen from these two species. Therefore, a detailed combined light- and scanning electron microscopy-based pollen-analysis of each taxon was conducted, the pollen was described, measured, and compared using statistical approaches and principal component analyses to establish unbiased results. The correlation-based principal component analysis achieved for each species shows an overall good superposition of pollen grains measured in equatorial and polar views in the first principal plane, revealing that the *P. persica* pollen is morphometrically as homogeneous as that of *P. subaequalis*. Then, the significant difference, mainly driven by lumen density, has been highlighted between the two species. Ultimately, the cross-validation of the resulting two-species linear discriminants classifier shows that based upon this reference dataset, (sub)fossil pollen grain can now be confidently assigned to either of the two species with an 85.8% correct-assignment rate. This opens new doors in the affiliation of fossil *Parrotia* pollen and suggests that previous pollen records need to be revised.

1. Introduction

Some areas of the northern Hemisphere were less impacted by the severe cold climate conditions of the Pleistocene glaciations (Frenzel et al., 1992). For that reason, particular areas in the temperate biome of Eurasia became refugia for several plant species referred to as Arcto-Tertiary floral elements (Manchester et al., 2009). Species such as *Zelkova carpinifolia* (Pall.) Dippel, *Parrotia persica* (DC.) C.A.Mey., *Pterocarya fraxinifolia* (Lam.) Spach, *Acer cappadocicum* Gled., and *Ginkgo biloba* L. are valid examples of relict plant taxa that nowadays occur in refugia regions in Iran (the Hyrcanian forest), on Crete (Greece) and Sicily (Italy), and in Eastern Asia. However, while these plants are important in characterizing the impact of the last glacial/interglacial cycles (Manchester et al., 2009; Akhani et al., 2010), the paleoclimatic and paleophytogeographic history of these relict species in their modern refugia is poorly understood (Cao et al., 2016). The lack of information is partly attributed to the scarcity of Cenozoic plant fossil records from the Caucasus prior to the Late Miocene (Shatilova et al., 2011). In addition, the difficulty in identifying tricolpate pollen of Hamamelidaceae is considered the cause of the absence of *Parrotia* in Eastern-Asia Cenozoic floras, a region which is now home to many Arcto-Tertiary floral elements (Zhi-chen et al., 2004). Moreover, due to the dampened effect of Quaternary glaciations the Arcto-Tertiary

☆ This study is dedicated to Professor Hossein Akhani in appreciation of his significant contribution to the flora and vegetation of the Hyrcanian forest.

* Corresponding author.
E-mail address: benjamin.adroit@gmail.com (B. Adroit).

https://doi.org/10.1016/j.revpalbo.2022.104776

elements persisted in their ecosystems and only developed slight morphological changes which might mask recent diversification events (Qian and Ricklefs, 2000; Nagalingum et al., 2011). Thus, a focus on the detection and characterization of morphological differences and variability between species of the same genus, from the past to present, will provide insights into the evolutionary history of these Arcto-Tertiary floral elements in response to for example, the formation of dispersal barriers and environmental changes.

Pollen is primordial for highlighting changes in plant taxa from both a chronological and chorological perspective (Marquer et al., 2014; Martin and Harvey, 2017). Morphological dissimilarities between pollen of closely related species may also reflect differences in the adaptation to long-term environmental changes (e.g. Cruden, 1976; Hedhly et al., 2005). Several paleoecological studies, especially from Europe, provide insight into Quaternary environments, vegetation, and climate (e.g., Leroy and Roiron, 1996; Reille et al., 2000), and some studies have focused on specific relict plant taxa, such as *Zelkova* (Follieri et al., 1986) and *Parrotia* (Bińka et al., 2003), from particular geographic regions. However, the limitation of the palynological approach is that pollen identification can usually be made only at the family and/or genus level and it can be hard or impossible to differentiate species or subspecies of the same genus (Nakagawa et al., 1998, for *Zelkova* spp.). For example, the pollen of *Zelkova* has been discovered from Quaternary sediments in most of Europe, and these pollen records could represent several different species, which some have gone extinct and/or are now relicts in Crete (Kozlowski et al., 2014) and Sicily (Garfì and Buord, 2012). The lack of ability to distinguish pollen from different sister species prevents reliable biogeographic studies related to paleoenvironmental changes. In that context, the case of the Persian ironwood (*Parrotia persica* (DC.) C.A.Mey) is of particular importance. *P. persica* (Hamamelidaceae) is one of the most noteworthy endemic relict tree species growing in the Hyrcanian forest (northern Iran and eastern Azerbaijan) (e.g. Yosefzadeh et al., 2010; Sattarian et al., 2011; Sefidi et al., 2011; Ramezani et al., 2013; Adroit et al., 2018, 2020). This forest refugium was recently declared a UNESCO World Heritage site due to its unique biodiversity including relic Arcto-Tertiary species such as *P. persica* (UNESCO, 2019). From a larger temporal perspective, the Persian ironwood has not been restricted to this geographic area and is well known from various Eurasian Cenozoic leaf and pollen records (e.g. Naud and Suc, 1975; Leroy and Roiron, 1996). The oldest European *Parrotia* pollen records date to the earliest Eocene (cf. Popescu et al., 2021, supplementary data) and fossil leaf records to the Early Miocene (Kvaček, 1998). The intensification of colder conditions in the late Cenozoic had a significant impact on the distribution and isolation of numerous Arcto-Tertiary floral elements (e.g. Suc and Popescu, 2005; DeChaine and Martin, 2006; Milne, 2006; Sagheb-Talebi et al., 2014), including *Parrotia persica* (Bińka et al., 2003; Jiménez-Moreno et al., 2010; Biltekin et al., 2015). *Parrotia* is a good example of genus distribution and speciation affected by glaciations, evidenced by the recent discovery of *Parrotia subaequalis* in mountain forests of Southeast China (Fig. 1) (Fang et al., 1997; Li et al., 1997, 2012; Zhang et al., 2018a). The late Cenozoic isolation of *Parrotia* populations led to differences in leaf morphology between the two extant species, Iran's *P. persica* and China's *P. subaequalis* (Plates I–II). It is thus important to also compare the pollen morphology of both species to note the impact of biogeographical isolation on their complete morphological traits. The similarities between the pollen of both taxa and the diagnostic features that segregate them are important to unravel the origin and evolution of these two species using the palynological record.

This study aimed to investigate whether morphological differences could be detected that segregate *P. persica* pollen from *P. subaequalis*. The combined light and scanning electron microscopy based pollen morphology of each taxon was described, measured in detail and compared using acknowledged statistical approaches and morphologically based principal component analyses to establish unbiased results. Based on the morphological traits of extant *Parrotia* pollen observed with LM, previously illustrated Eurasian fossil pollen grains were re-measured and compared to the range noted for pollen from the two extant species. The detected change in pollen morphology over time is further discussed in relation to both climatic as well as biogeographic evolution in both time and space throughout the Cenozoic.

2. Material and methods

2.1. Origin and accessibility of samples

Pollen from both extant *Parrotia*, freshly collected as well as herbarium material was analyzed. Flowers were collected from trees occurring in their natural habitats, *Parrotia persica* flowers from plants in the Hyrcanian forest of Iran, and *P. subaequalis* flowers from plants in the Yixing forest of eastern China. The herbarium material used for this study belongs to the following collections: 1) Herbarium of the Department of Paleontology of the University of Vienna (HDP-WU); 2) IMBE palynological database, CNRS, Aix-Marseille University (MEPRC); 3) ISEM reference palynological database, CNRS, University of Montpellier.

2.2. Sample preparations

The anthers were extracted from the flowers and acetolyzed following the protocol called 'fast way' of Halbritter et al. (2018, p. 103). Individual grains were then photographed with light microscope (LM) and transported onto scanning electronic microscope (SEM) stubs to be photographed following the "single-grain method" as modified by Halbritter et al. (2018, p. 121).

2.3. Pollen observations, descriptions, and measurements

Pollen grains were observed with both LM and SEM and described and measured following Punt et al. (2007) and Halbritter et al. (2018). The morphometric characteristics of *P. persica* and *P. subaequalis* were established based on measurements with LM from 120 pollen grains: 60 for each species, including 30 pollen grains measured in equatorial view and 30 in polar view (detailed measures are available in Suppl. 1).

2.4. Statistical analyses of pollen features

Due to previously observed differences in lumen size in *P. persica* pollen leading to the assumption of some polymorphism (Naud and Suc, 1975; Bińka et al., 2003; Paridari et al., 2012), and due to the larger lumen size in *P. subaequalis* pollen, a morphometric study was performed on pollen grains in both equatorial and polar views. Using a calibrated square (side = 10 μm) sketched on pollen photographs at magnification ×1000, the lumina were counted and thirty lumina measured in equatorial and polar views for each species. The morphometric characterization of *P. persica* and *P. subaequalis* pollen was assessed using complementary multivariate statistical tools based on the six quantitative descriptors (detailed measures are available in Supplement 1). All analyzes were performed using PAST v. 4.02 (Hammer et al., 2001). As a preliminary step, these 6 quantitative descriptors measured for each of the 120 pollen grains included in the analyzed dataset were first transformed in order to optimize within-species multivariate normality (evaluated using the Doornik-Hansen test; (Doornik and Hansen, 1994) and homoscedasticity (i.e., homogeneity of variances and co-variances, as evaluated using the Box's M test; (Rencher and Christensen, 2012) (Tables 1 and 2). The linear measurements (E, Lll, Wll, Lsl and Wsl, see caption Table 1) were log10-transformed, and the Nlumen (see caption Table 1) was square root-transformed, as customarily done for linear and count measurements, respectively (Sokal and Rohlf, 1995).

Fig. 1. Geographic maps showing the distribution of *Parrotia persica* in Iran and *P. subaequalis* in China. Distribution of extant populations marked with red based on (Sefidi et al., 2011; Zhang et al., 2018b; Liu et al., 2021). Geographic background adjusted from: *The World Factbook*, Central Intelligence Agency. (For interpretation of the references to color in this figure legend, the reader is referred to the web version of this article.)

Plate I. *Parrotia persica* in its natural habitat in the Hyrcanian forest, Iran. (1) Fruits, usually less than 1 cm in diameter. (2) Flowers, usually 1 cm long. (3–4) Leaves, oblong to obovate, commonly 10 cm in length, can reach 15 cm. (5–6) Tree or sometimes large shrub, usually 8–10 m tall, but can be up to 25 m. Scale bar = 1 cm in 1–4; 1 m in 5 and 6. Photos (1) from Dr. Hamid Gholizadeh; (2–4) from the open access website ebben.nl.

2.5. Principal component analysis

The multivariate distribution of pollen grains measured in equatorial and polar views was first explored separately for each species through correlation-based principal component analysis (PCA; Legendre and Legendre, 2012). Differences between the two views were further investigated through one-way Multiple Analysis of Variances (MANOVA; Rencher and Christensen, 2012) and its nonparametric equivalent, one-way PerMANOVA based on the Mahalanobis generalized distance matrix, 99.999 permutations; (Anderson, 2001). These tests were coupled with two-group linear discriminant analysis (LDA; Legendre and Legendre, 2012) in order to visualize group differences

Plate II. *Parrotia subaequalis* in its natural habitat in the Yixing forest, China. (1) Flowers, usually 1 cm in length. (2) Fruits, between 0.7–1 cm in diameter. (3–4) Leaves, broad-obovate, 4–6.5 cm long and 2–4.5 cm wide. (5–6) Small tree or large shrub, 5–10 m tall. Scaler bar = 1 cm in 1–4; 1 m in 5, 6. Photos (1–3) from te open access website ebben.nl.

along the canonical axis tested by MANOVA. Additionally, the multivariate difference of the two species in both equatorial and polar views was evaluated using two-group one-way MANOVA (two species) and four-group one-way MANOVA (two species × two views). The same two-group and four-groups were conducted on a one-way and two-way Mahalanobis-based PerMANOVA coupled with the corresponding LDA.

2.6. Climatic and biome niche analysis

We compiled historical climate data (1970–2000) from 196 georeferenced occurrences of *P. persica* and seven of *P. subaequalis* using WorldClim vers. 2.1 (https://www.worldclim.org/data/worldclim21.html) at a resolution of 30 s (ca. 1km^2; Fick and

Table 1
Light microscopy measurements of *Parrotia* pollen.

	E (in μm)	Nlumen	Lll (in μm)	Wll (in μm)	Lsl (in μm)	Wsl (in μm)
P. persica, equatorial view						
Pollen number	30	30	30	30	30	30
Mean ± Std.Dev.	36.06 ± 6.763	53.0 ± 15.27	1.25 ± 0.219	0.76 ± 0.177	0.70 ± 0.130	0.59 ± 0.123
Median [1st–3rd Quartile]	33.75 [30.68–41.78]	52.75 [42.5–67]	1.2 [1.1–1.3]	0.7 [0.6–0.9]	0.7 [0.6–0.8]	0.55 [0.5–0.7]
Min–Max values	27.5–53.4	26.5–91.5	0.9–2	0.5–1.2	0.5–1	0.4–0.8
P. persica, polar view						
Pollen number	30	30	30	30	30	30
Mean ± Std.Dev.	38.44 ± 6.597	64.3 ± 15.51	1.24 ± 0.247	0.76 ± 0.138	0.64 ± 0.116	0.54 ± 0.101
Median [1st–3rd Quartile]	36 [33.08–44.48]	65.75 [52.8–72.6]	1.25 [1–1.43]	0.8 [0.7–0.8]	0.65 [0.5–0.7]	0.5 [0.5–0.6]
Min–Max values	26.9–48.9	35–105.5	0.9–1.8	0.5–1.1	0.4–0.8	0.4–0.8
P. subaequalis, equatorial view						
Pollen number	30	30	30	30	30	30
Mean ± Std.Dev.	30.16 ± 2.751	46.7 ± 12.85	1.72 ± 0.567	0.86 ± 0.299	0.83 ± 0.202	0.71 ± 0.172
Median [1st–3rd Quartile]	30.05 [29.0–32.65]	43 [36–57]	1.6 [1.3–2]	0.8 [0.675–0.9]	0.8 [0.7–1]	0.7 [0.6–0.8]
Min–Max values	22.8–34.5	27.5–79	1–3.5	0.6–1.8	0.4–1.2	0.4–1.1
P. subaequalis, polar view						
Pollen number	30	30	30	30	30	30
Mean ± Std.Dev.	30.32 ± 3.253	44.6 ± 11.17	1.96 ± 0.491	0.95 ± 0.354	0.84 ± 0.194	0.69 ± 0.157
Median [1st–3rd Quartile]	30.55 [29.1–32.03]	44.5 [34.5–54.5]	1.9 [1.6–2.3]	0.8 [0.7–1.25]	0.8 [0.7–0.93]	0.7 [0.6–0.8]
Min–Max values	23–36.1	25–72	1–2.9	0.5–1.6	0.5–1.2	0.4–1.1

Note: Statistical summary of the six quantitative descriptors measured for *P. persica* and *P. subaequalis* in equatorial and polar views (see Suppl. 1 for full detailed values). E (μm) = equatorial diameter of pollen. Nlumen = number of lumina per 10 μm^2 of pollen surface, which corresponds to the lumen density in fine. Lll and Wll = length and width of the largest lumen observed in the same 10 μm^2 area. Lsl and Wsl = length and width of the smallest lumen observed in the same 10 μm^2 area.

Hijmans, 2017; see Supplementary File 2). The georeferenced data were filtered so that multiple occurrences with the same coordinates were treated as a single data point. To characterize climatic and ecological niches of the two modern species, we created distribution maps for each species using the GBIF dataset (https://www.gbif.org/). These occurrences were plotted onto 5 arc minutes grid Köppen-Geiger climate maps (1986–2010 data; Kottek et al., 2006; Rubel et al., 2017) to establish "Köppen signatures" for both species; and on major terrestrial biome maps (Olson et al., 2001) to assess their biome preferences. For the Köppen-Geiger plots, the georeferenced datasets were filtered so that multiple occurrences in a single grid cell were only counted once (labeled 'unique grid cells' in the diagrams; Supplementary File 3). Likewise, for the biome plots, georeferenced data were filtered so that multiple occurrences within the same coordinates were treated as single data points (labeled 'unique localities' in the diagrams; Supplementary File 3). Georeferenced data and the Köppen-Geiger maps with a 5 arc minutes resolution were processed using the "Sample Raster Values" Toolbox in QGIS Version 3.16.4-Hannover. The biome shape files were processed using the "Geoprocessing Tool" intersection in QGIS. The biomes and Köppen-Geiger climates occupied by both *Parrotia* species are shown as maps generated with QGIS and as frequency (proportional distribution) diagrams (Supplementary File 3). Excel files provide the raw point data (Supplementary File 2).

3. Results

3.1. Pollen descriptions

Species: Parrotia persica (DC) C.A.Mey. (Tables 1 and 2; Plates III and V).

Description: Monad, oblate to prolate, spheroidal, circular to semi-lobate in polar view, elliptic to semi-circular in equatorial view; tricolpate; exine 2–2.5 μm thick, nexine thinner than sexine; semitectate; reticulate, heterobrochate; microreticulate, with nanoechinate suprasculpture in SEM; muri narrow, 0.3–0.6 μm wide, rounded, often incomplete in intercolpium (SEM); nanoechini mostly in single rows; lumina (i.e., perforations) small, 0.1–1.5 μm wide, circular to irregular in outline, with few (0–4) freestanding columellae, lumina decreasing sharply around colpi (SEM); colpus membrane echinate to nanoechinate and granulate, sculpture elements conglomerating along colpus margin forming irregular and segmented verrucae to rugulae with nanoechinate suprasculputre (SEM).

Remarks: *Parrotia persica* pollen has previously been studied with both LM (Naud and Suc, 1975; Paridari et al., 2012) and SEM (Bogle and Philbrick, 1980; Fritz and Allesch, 1999; Bińka et al., 2003; Paridari et al., 2012).

Parrotia subaequalis (Hung T.Chang) R.M.Hao et H.T.Wei (Tables 1 and 2; Plate IV and VI).

Table 2
Multivariate statistical tests and morphometrical characterization of *Parrotia* pollen.

	P. persica	*P. subaequalis*	*P. persica* vs. *P. subaequalis*	*P. persica* vs. *P. subaequalis*
	Equatorial vs. polar views	Equatorial vs. polar views	(two groups, pooled views)	(four groups, separate views)
Multivariate normality (Doornik-Hansen)	Ep = 7.8; p = 0.80 NS	Ep = 15.2; p = 0.23 NS	Ep = 24.4; p = 0.018 *	Ep = 24.4; p = 0.018 *
Multivariate Homoscedasticity (Box's M)	M = 24.3; p = 0.42 NS	M = 34.0; p = 0.088 NS	M = 73.6; p = 4.1×10^{-7} ***	M = 124.8; p = 1.1×10^{-4} ***
One-way MANOVA (Wilks λ)	λ = 0.77; p = 0.027 *	λ = 0.92; p = 0.59 NS	λ = 0.43; p = 1.4×10^{-18} ***	λ = 0.35; p = 2.7×10^{-17} ***
One-way PerMANOVA (Mahalanobis)	F = 2.30; p = 0.028 *	F = 0.79; p = 0.59 NS	F = 12.30; p < 10^{-5} ***	F = 5.40; p < 10^{-5} *** Species: F = 12.52; p < 10^{-5} ***
Two-way PerMANOVA (Mahalanobis)	–	–	–	View: F = 2.31; p = 0.028 * Interaction: F = 1.37; p = 0.22 NS

Note: In each case, the statistics is given, followed by its corresponding p-value (p). NS is used for Non-Significant result; Ep and M are the respective names of the Doornik-Hansen and Box's M statistical test result. NS: p > 0.05 (non-significant); *: 0.01 < p < 0.05 (weakly significant); **: 0.001 < p < 0.01 (moderately significant); ***: p < 0.001 (strongly significant).

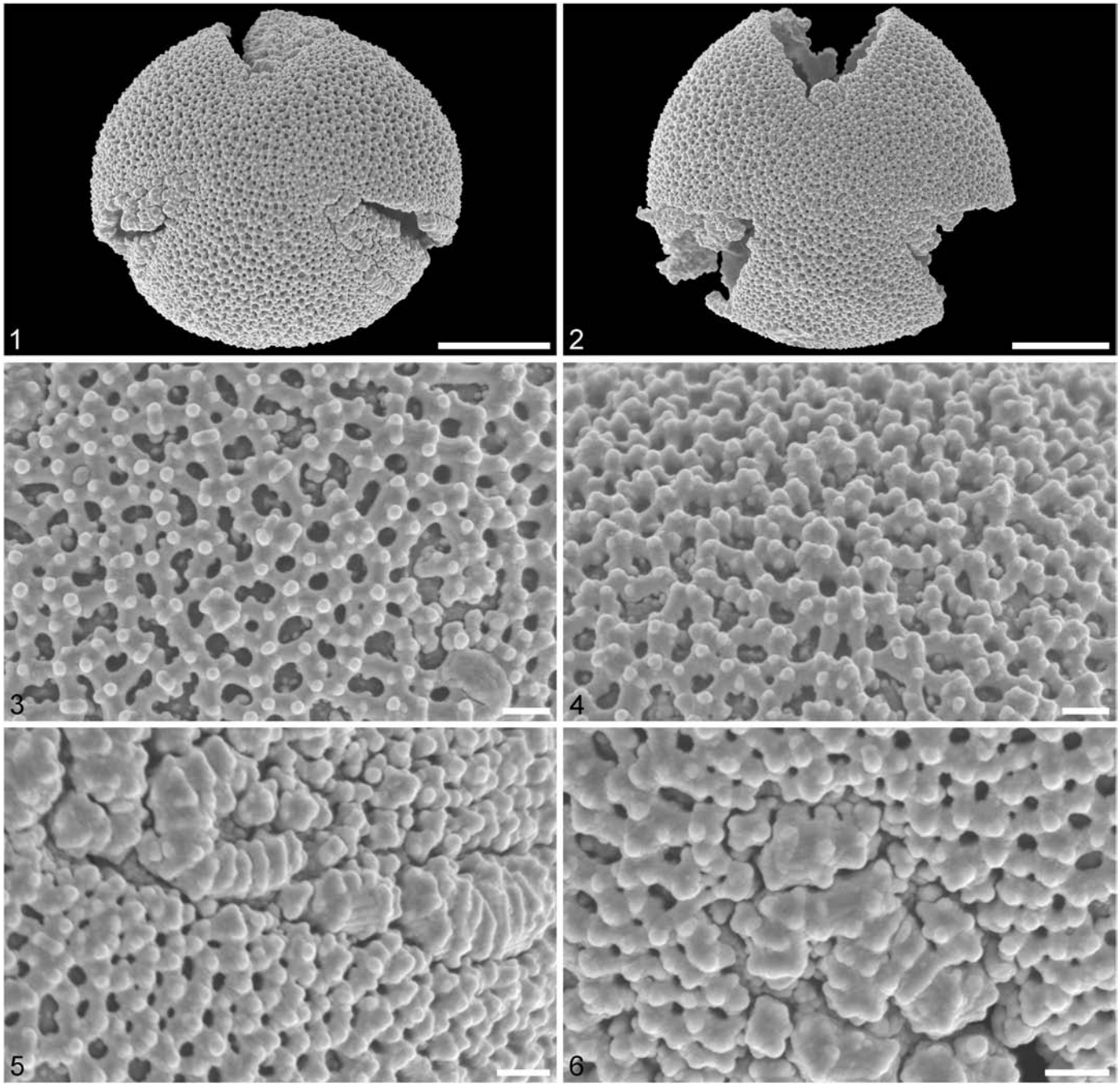

Plate III. Scanning electron microscopy (1–6) micrographs of *Parrotia persica* (from North Iran, coll. M.A. Fischer, s.n. [HDP-WU]. (1) Polar view, aperture membrane preserved. (2) Polar view, aperture membrane mostly lost. (3) Close-up of central polar area. (4) Close-up of interapertural area. (5) Close-up showing colpus margin and membrane. (6) Close-up showing the end of the colpus and membrane. Scale bars – 10 μm (1–2), 1 μm (3–6).

Description: Monad, oblate, spheroidal, circular to semi-lobate in polar view, elliptic to semi-circular in equatorial view; tricolpate; exine 1.2–2 μm thick, nexine thinner than sexine; semitectate; reticulate, heterobrochate, with nanoechinate suprasculpture in SEM; muri narrow, 0.5–0.8 μm wide, rounded, often incomplete in intercolpium (SEM); nanoechini mostly in single rows; lumina small to large, 0.6–2.5 μm wide, circular to irregular in outline, with few to many (0–12) free-standing columellae, lumina decreasing sharply around colpi (SEM); colpus membrane echinate to nanoechinate and granulate, sculpture elements conglomerating along colpus margin forming irregular verrucae with nanoechinate suprasculputre (SEM).

3.2. Statistical approach and pollen comparison

The correlation-based PCA achieved for each species show an overall good superposition of pollen grains measured in equatorial and polar views in the first principal plane (explaining 61.7% and 67% of the total variability for *P. persica* and *P. subaequalis*, respectively; Fig. 2A, C). In both cases, the multivariate space appears to be structured in the same way, with the lumen density vs. size of the smallest and largest lumina driving the first principal component, and the equatorial diameter driving the second principal component. Parametric and nonparametric MANOVAs confirm for each

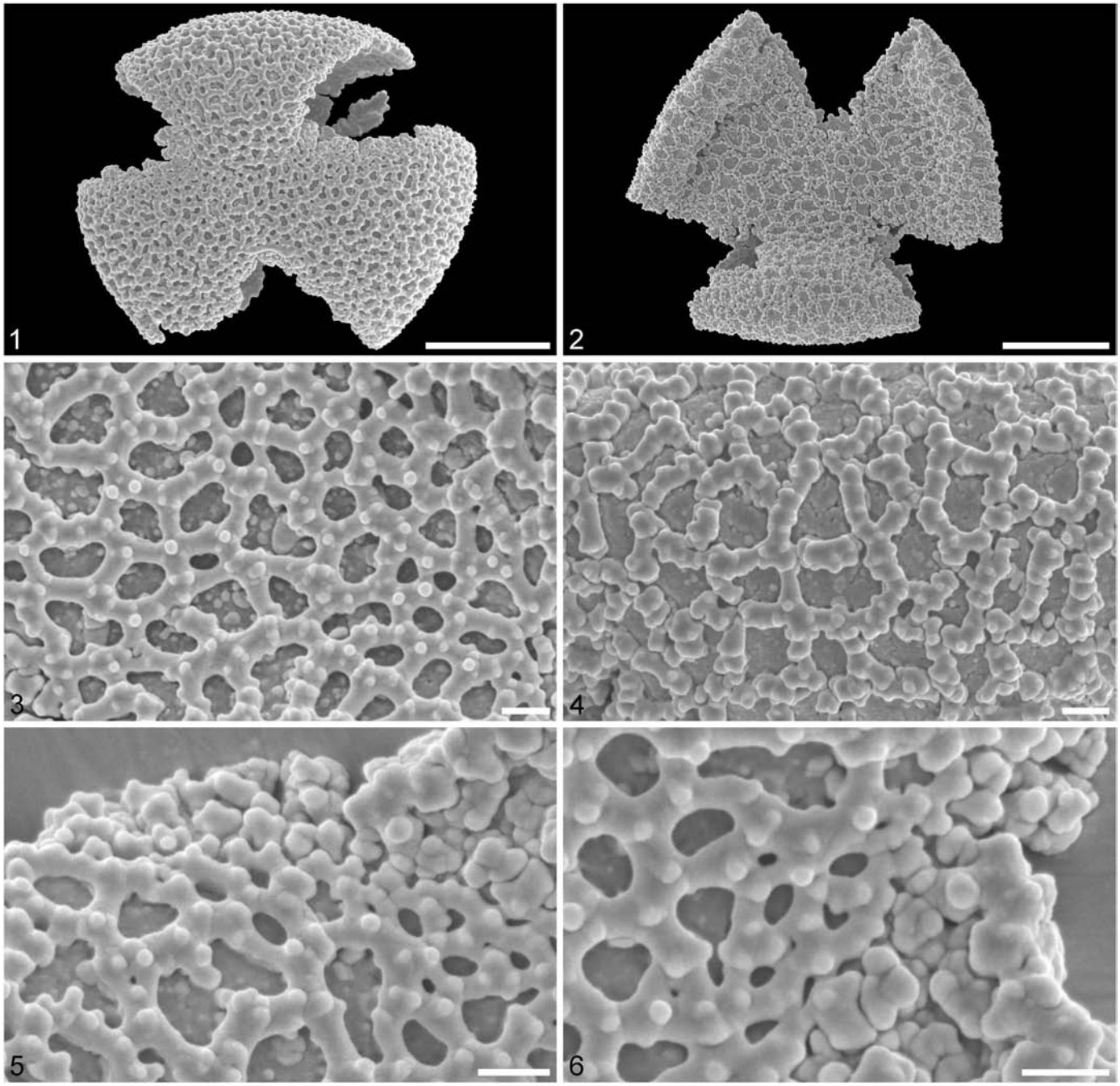

Plate IV. Scanning electron microscopy (1–6) micrographs of *Parrotia subaequalis* (slide MEPRC-1050 of the IMBE collection, plant sample collected in China). (1) Polar view, partly preserved aperture membrane. (2) Polar view, aperture membrane mostly lost. (3) Close-up of central polar area. (4) Close-up of interapertural area. (5) Close-up showing colpus margin and membrane. (6) Close-up showing the end of the colpus and membrane. Scale bars – 10 μm (1–2), 1 μm (3–6).

species the impossibility of distinguishing between specimens observed in the equatorial view and those observed in the polar view (Table 1). The significant result obtained for *P. persica* is a spurious by-product of the presence in the analyzed sample of 22 (37%) large-E pollen grains (equatorial diameter) pollen grains coming from a single microscope slide (n° 35,249) and involving 13/22 (59%) grains in polar view, while the small-E group involves 17/38 (44.7%) grains in polar view. Similar tests achieved without the equatorial diameter descriptor return non-significant results confirming the morphometric homogeneity between equatorial and polar views (MANOVA: $\lambda = 0.86$, $p = 0.13$ NS; PerMANOVA: $F = 1.69$, $p = 0.13$ NS). Finally, the two-group LDA (Linear Discriminant Analysis) illustrates the lack of morphometric differences between equatorial and polar views for each species (Fig. 2B, D).

On the contrary, compared to each other, pollen from the two *Parrotia* species show highly significant morphometric differences based on pooled and separate equatorial and polar views (Table 2). The two-way PerMANOVA (species × view) confirms that most of the morphometric heterogeneities between groups come from differences between species, with no significant interaction between species and view factors. The corresponding LDAs also illustrate significant differences, showing that the morphometric difference between the two species is mainly driven by lumen density vs. size of the smallest and largest lumina (Fig. 3).

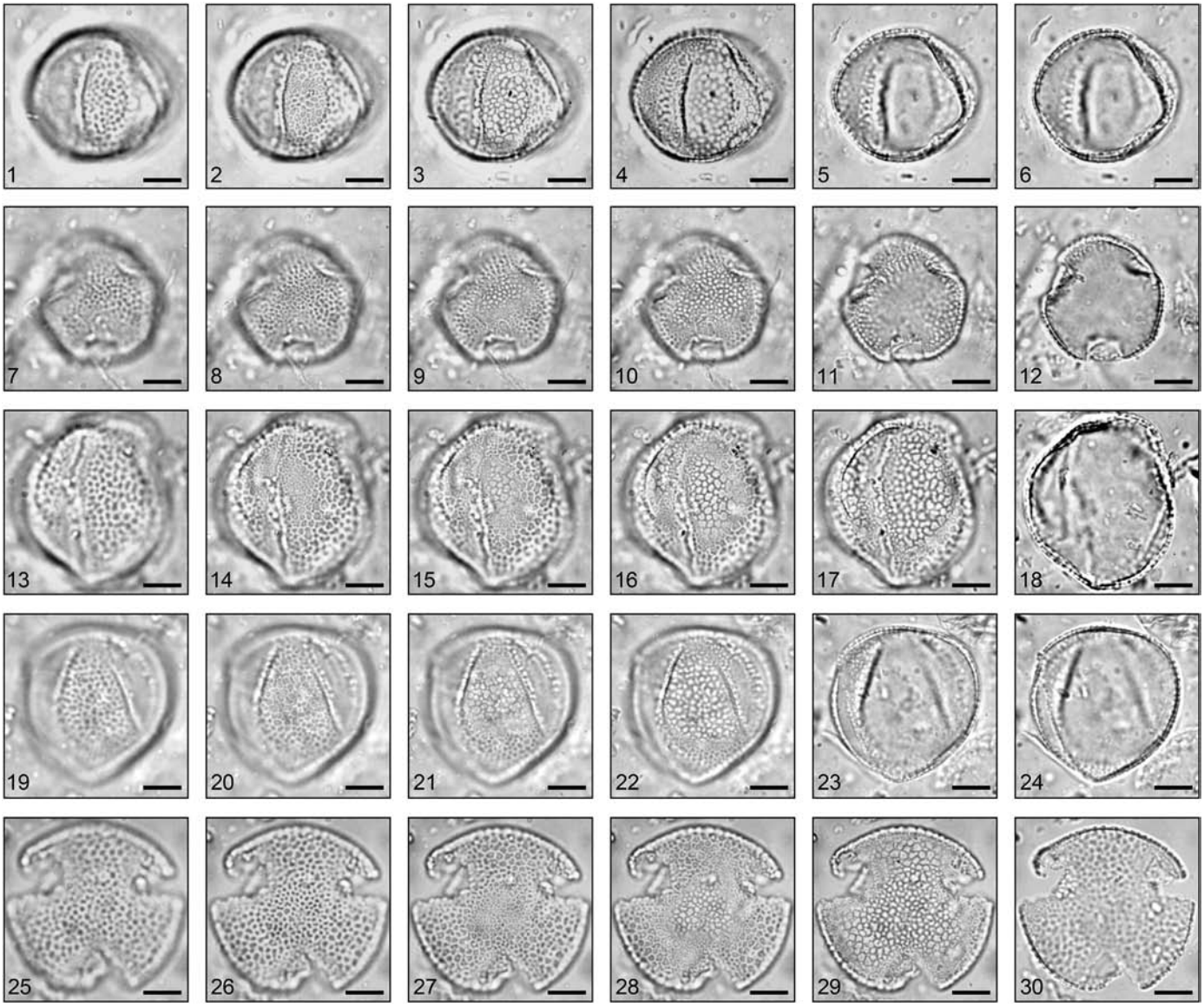

Plate V. *Parrotia persica* C.A.Mey, modern pollen grain (slide 20407 of the ISEM collection, plant specimen collected in Iran). 1–6, Pollen in equatorial view (aperture facing), L.O. analysis: 1, surface of reticulate ornamentation; 2, base of lumina; 3, foot of columellae; 4–5, colpi; 6, optical section. 7–12, Pollen in polar view, L.O. analysis: 7, surface of reticulate ornamentation; 8, base of lumina; 9, foot of columellae; 10–11, colpi; 12, optical section. 13–18, Pollen in equatorial view (aperture facing), L.O. analysis: 13, surface of reticulate ornamentation; 14, base of lumina; 15, foot of columellae; 16–17, colpi; 18, optical section.
19–24, Pollen in equatorial view (intercolpium facing), L.O. analysis: 19, surface of reticulate ornamentation; 20, base of lumina; 21, foot of columellae; 22–23, colpi; 24, optical section. 25–30, Pollen in polar view, L.O. analysis: 25, surface of reticulate ornamentation; 26, lumina; 27, base of lumina; 28, foot of columellae; 29, colpi; 30, optical section. Scale bar = 10 μm.

3.3. Extant Parrotia biomes and climate niches

Both extant *Parrotia* species are part of the "Temperate Broadleaf and Mixed Forests" biome (Olson et al., 2001; Supplementary File 3). Based on our georeferenced dataset, both species display relatively similar mean annual temperature (MAT) preferences and coldest month mean temperature (CMMT) tolerances (Supplementary Files 2 and 3). Significant differences were observed with precipitation. While *P. subaequalis* thrives under fully humid conditions (Cfa climate; Fig. 4), with 1052 (1287) 1585 mm mean annual precipitation (MAP) and 485 (549) 666 mm of precipitation during the three warmest month, *P. persica* tolerates 291 (750) 1195 mm MAP, with strong seasonality and a precipitation depression during the summer months. With only 22 (76) 135 mm of precipitation during the three warmest months, *P. persica* thrives mainly under a Csa climate (Fig. 4), bordering in the east of its natural distribution to BS climate and extending at higher elevations along the mountain ranges near the Caspian Sea into Cfa climate.

4. Discussion

4.1. Concrete distinction of pollen

The pollen of both *Parrotia* species is easily identified at the genus level. The suspected polymorphism of *P. persica* pollen can be rejected based on the LDA, revealing that the *P. persica* pollen is morphometrically as homogeneous as those of *P. subaequalis*. When compared, the pollen grains of *P. persica* are slightly larger and their exine is thicker than those of *P. subaequalis* (Plates III and IV; Tables 1 and 2). Although pollen grains of both species are reticulate in LM, the lumen density is much finer in *P. persica* than in *P. subaequalis*. These differences are more visible with SEM observations, where the sculpture of *P. persica* is micro-reticulate and the sculpture of *P. subaequalis* is reticulate (compare Plate III, 3 and 4 to Plate IV, 3 and 4). SEM further differentiates the reticulate sculpture of the two species; the muri are broader, the diameter of the lumina is larger, and the number of free-standing columellae

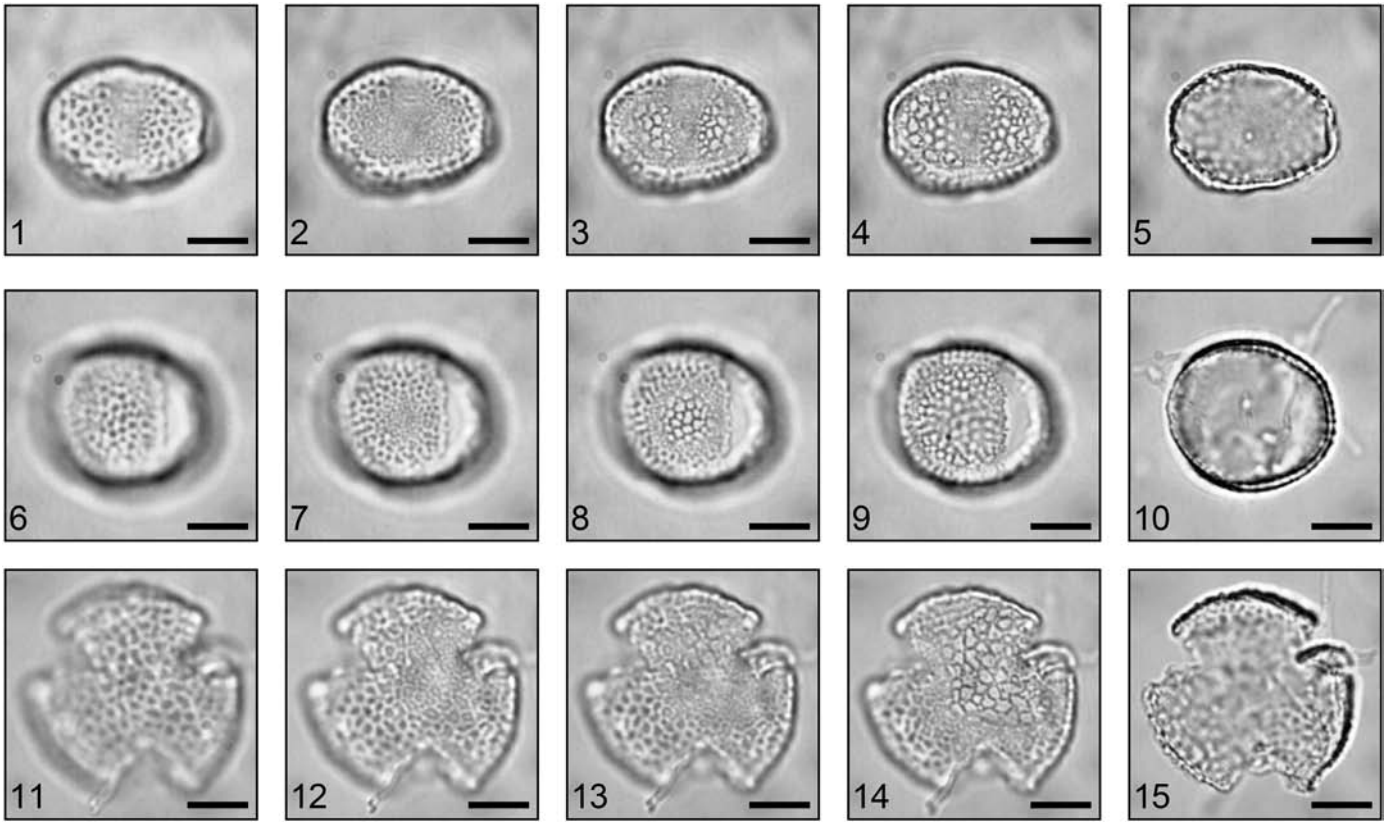

Plate VI. *Parrotia subaequalis* (Hung T.Chang) R.M.Hao & H.T.Wei, modern pollen grain (slide 941 of the Geobiostratdata collection, plant specimen collected in China). 1–5, Pollen in equatorial view (aperture facing), L.O. analysis: 1, surface of reticulate ornamentation; 2, base of lumina; 3, foot of columellae; 4, colpus; 6, optical section. 6–10, Pollen in equatorial view (intercolpium facing), L.O. analysis: 6, surface of reticulate ornamentation; 7, base of lumina; 8, foot of columellae; 9, colpi; 10, optical section. 11–15, Pollen in polar view, L.O. analysis: 11, surface of reticulate ornamentation; 12, lumina; 13, foot of columellae; 14, colpi; 15, optical section. Scale bar = 10 μm.

is higher in *P. subaequalis* compared to *P. persica*. Furthermore, sculpture elements along the colpus margins are differently arranged in the two species (compare Plate III, 5 and 6 to Plate IV, 5 and 6). Furthermore, statistical approaches confirm the significant difference between pollen of the two *Parrotia* species. Combining the available evidence, *P. persica* is best characterized by a dense and small lumina, while *P. subaequalis* is characterized by a less dense and larger lumina, as summarized in Table 1. Ultimately, the cross-validation of the resulting two-species linear discriminant classifier shows that based on this reference dataset, (sub)fossil pollen grains can now be confidently assigned to either one of the *Parrotia* species with an 85.8% correct-assignment rate.

4.2. Inputs for paleopalynology and affiliation to extant species

The equatorial diameter (E) and length of the polar axis (P) in fossil *Parrotia* pollen is usually not comparable to that of pollen from extant *Parrotia* due to the hydrated state of extant material studied with LM. Potential fossil *Parrotia* pollen is mostly preserved in dehydrated state, either with the aperture enfolded or widely open (lacking colpus membrane). Fossil pollen grains with enfolded apertures are stretched along their polar axis, therefore, they have an excessively long polar axis compared to their equatorial diameter. Grains with widely open apertures are collapsed, and their poles are compressed; therefore, they have an excessively wide equatorial diameter. This makes it hard to compare the size/outlines/shape (e.g. the P/E-ratio) of single dispersed fossil *Parrotia* pollen to that of either *P. persica* or *P. subaequalis*. Irrelevant to this is the sculpture observed in LM and/or SEM. The number and size of the lumina are not affected by the P/E ratio and can be measured in both fossil and extant pollen and compared. As evident in Table 1, there is a clear difference in the lumen size range and partly in their number per 10μm^2 between the two living species. These features currently seem to be the only tool for possibly segregating fossil *Parrotia* pollen and investigating if they are morphologically/taxonomically closer to one or the other extant species. To test this, we measured the lumen features from potential fossil dispersed *Parrotia* pollen previously described from Late Oligocene to Pliocene localities of Europe (see Table 3, and references therein). Interestingly, the oldest European records from our comparison, which are of late Oligocene to Middle Miocene age, suggest affiliation to *P. persica*. The younger records, of Late Miocene to Pliocene age, suggest affiliation to *P. subaequalis*. The reasons for this might be as follows: 1) the pollen type of *P. persica* is the basal/ancestral pollen within *Parrotia*, and European Oligocene to Middle Miocene *Parrotia* plants, one species or more, produced pollen comparable to that of modern-day *P. persica*. The change or addition in morphology could reflect a divergence within the genus and the origin of a new species that is now confined to East Asia; 2) this has no meaning and the affiliation 'older versus younger records' to either of the living species might change and intertwine back in time when a larger number of records are considered. I any case, such assumptions would have to be supported or rebutted in a future more detailed study based on a larger fossil pollen collection from different Eurasian locations.

4.3. Paleoecological and paleoclimatological considerations

Since plant species of the same genus can characterize drastically different ecological niches, it is important to be able to segregate tree pollen at intrageneric levels, especially when those taxa are also present in the fossil record. For example, the genus *Acer* comprises more than hundred different plant species developing within drastic different environments. In western Eurasia (Europe, Caucasus), pollen cannot be

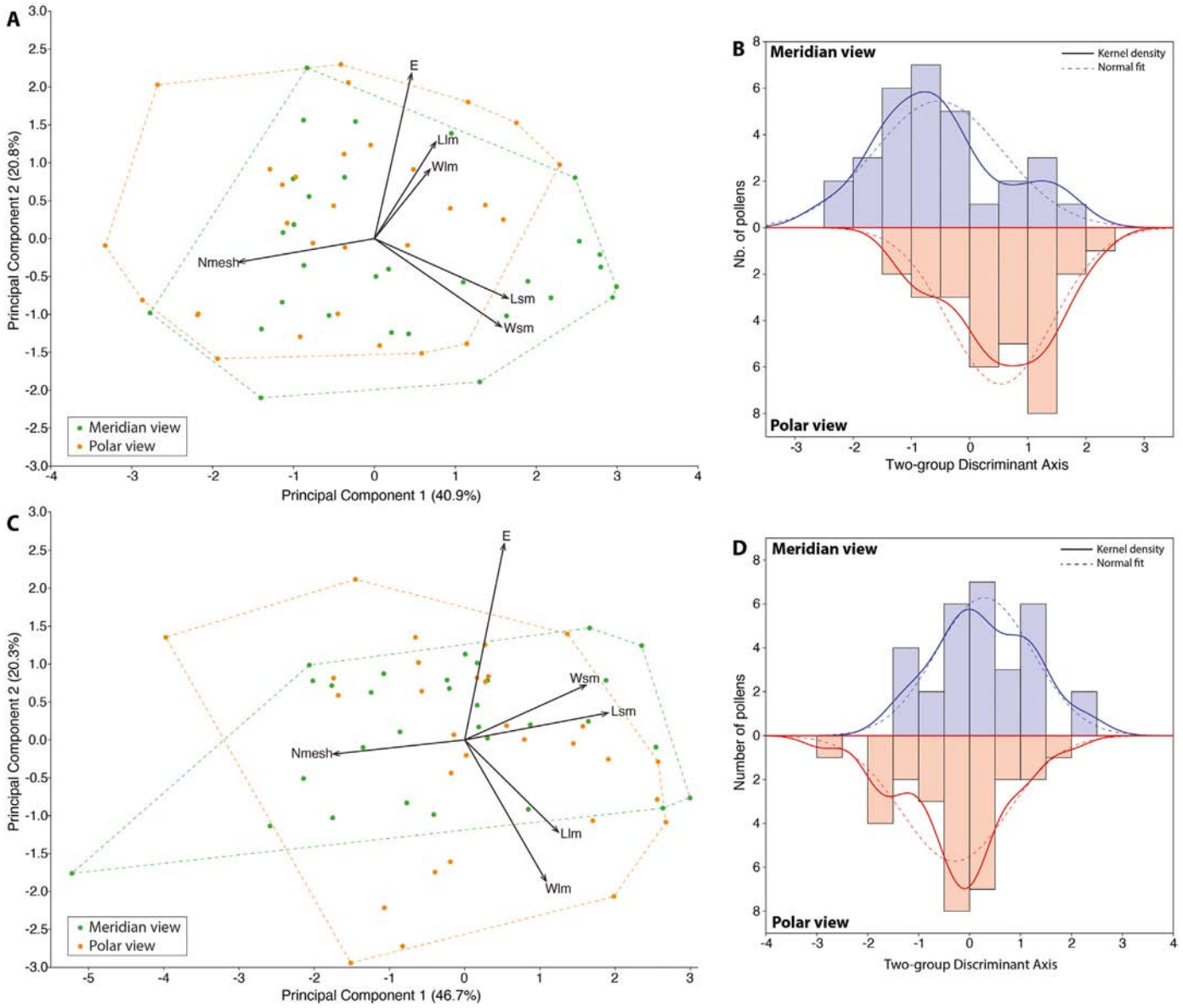

Fig. 2. Principal Component and Linear Discriminant Analyses of *Parrotia* pollen. Correlation-based Principal Component Analyses (A, C) and two-group (equatorial view vs. polar view) Linear Discriminant Analyses (B, D) of 60 pollen grains from *Parrotia persica* (A, B) and *P. subaequalis* (C, D).

used to discriminate between the drought-adapted *Acer monspessulanum* L., *Acer campestre* L., *Acer cappadocicum* Gled., which occupy a closed montane forest even up to a mesic valley (Akhani, 1998), and the humid forest species such as *Acer velutinum* Boiss., *Acer pseudoplatanus* L., *Acer platanoides* L. (Beug, 2004, p. 250). Another example is *Quercus*, also very widespread in the world and in the fossil record. The *Quercus robur-pubescens* pollen type cannot be discriminated between various white oaks that can be swamp forest or dry steppe forest elements (Beug, 2004, p. 144). However, the possibility to discriminate the evergreen (e.g., *Quercus ilex*-type) from deciduous oak (*Quercus robur*-type) has been an asset for paleoecologists to understand the ecological history of Mediterranean forest ecosystems.

As evident herein, *Parrotia* is one of those genera in which it is possible to differentiate between the pollen of its species. The case of *Parrotia* is interesting because this Arcto-Tertiary floral element can be useful in determining Quaternary interglacial paleo-refugia. So far, *Parrotia* pollen grains described from the Cenozoic of Eurasia have mostly been attributed to *P. persica* (Stachurska et al., 1973; Naud and Suc, 1975; Leroy and Roiron, 1996; Jiménez-Moreno et al., 2007; Jiménez-Moreno and Suc, 2007; Suan et al., 2017; Suc et al., 2020; Popescu et al., 2021). The present study shows that previous fossil pollen records could potentially be revised based on the pollen morphology and that future studies comprising fossil *Parrotia* pollen need to consider the morphological differences between the two extant species of the genus.

The main reasons why it is important to revise previous fossil *Parrotia* pollen records and correctly affiliate new finds is the potential impact on paleoenvironmental interpretations. Today, *P. persica* and *P. subaequalis* do not share the same bioclimatic conditions. Although their biomes can both be defined as Temperate Broadleaf & Mixed Forests, the climate sustaining *P. subaequalis* is a fully humid warm temperate climate with hot summers, a typical Cfa climate (e.g., Kottek et al., 2006; Fig. 4), while in the Hyrcanian forest, *P. persica* thrives under a warm temperate climate with hot but dry summers, a typical Csa climate (e.g., Kottek et al., 2006; Fig. 4, Supplementary Files 2 and 3). This difference in the present climatic conditions is also supported by the Computerized Bioclimatic Maps of the World (Rivas Martinez et al., 2011) where *P. persica* is shared between the bioclimate n°33

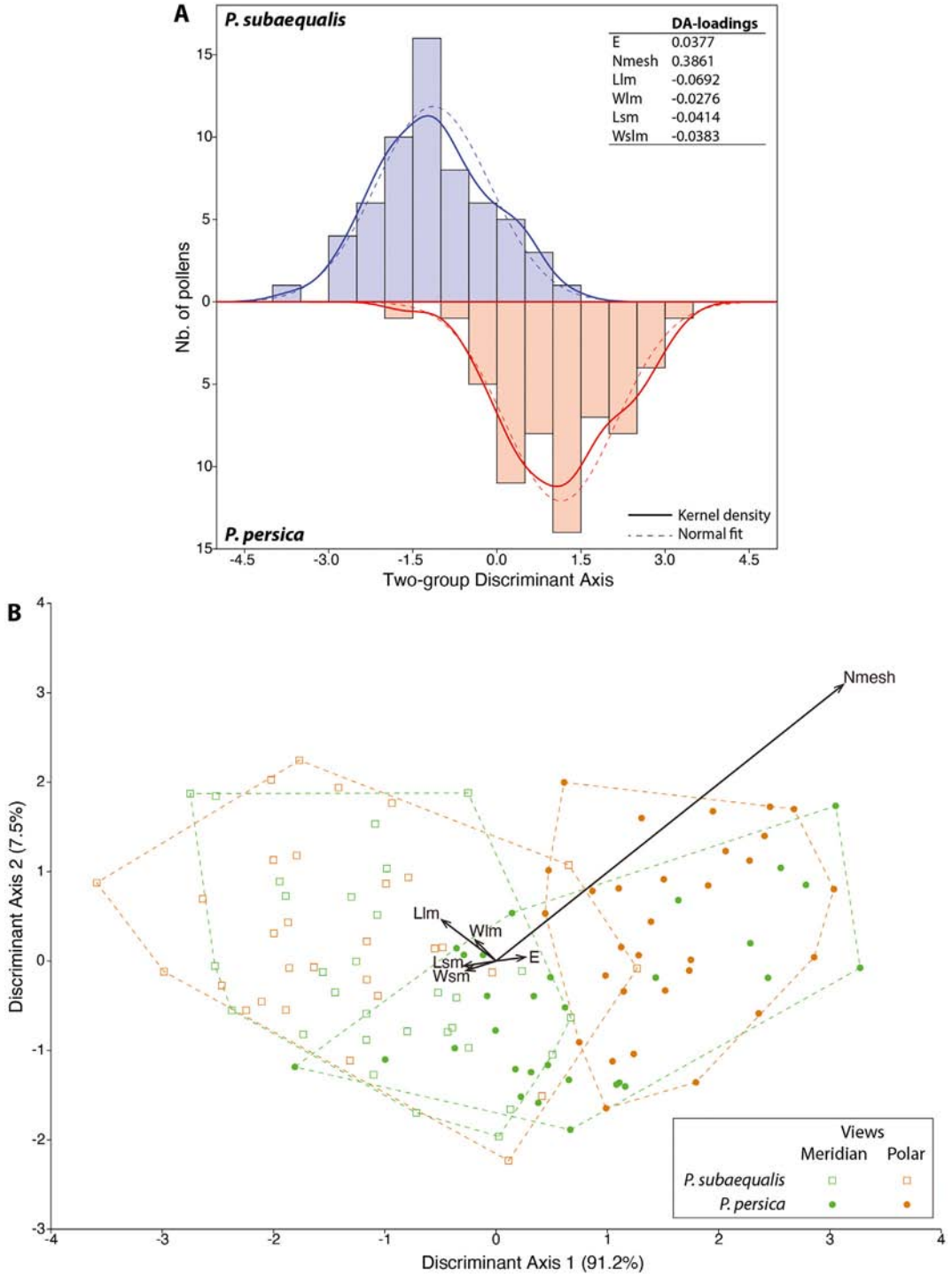

Fig. 3. Morphometric analyses of *Parrotia* pollen. Two-species (A) and four-group (2 species × 2 views; B) Linear Discriminant Analyses reflecting the morphometrical difference between *Parrotia persica* and *P. subaequalis*.

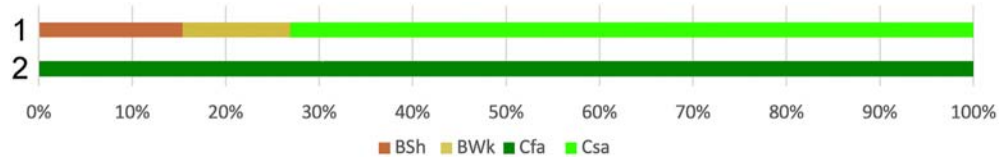

Fig. 4. Köppen-Geiger climate signatures of *Parrotia persica* and *P. subaequalis* based on their modern distribution. Climate types according to Kottek et al. (2006), Peel et al. (2007), and Rubel et al. (2017).

Table 3
Potential *Parrotia* pollen records and their affiliation.

Extant taxa	Distribution / Locality	Age	E (µm)	P (µm)	Nlumen (eq.v.)	Nlumen (p.v.)	Lll (eq.v.)	Lll (p.v.)	Wii (eq.v.)	Wii (p.v.)	Reference	Note on affiliation
Parrotia persica	Azerbaijan, Iran	Extant	26.9-**53.4**	21.3-26.3	26.5-**91.5**	35-**105.5**	0.9-2.0	0.9-1.8	0.5-1.2	0.5-1.1	This study	NA
Parrotia subaequalis	Southeast China	Extant	22.8-36.1	18.8-25	27.5-79	25-72	1-**3.5**	1.0-**2.9**	0.6-**1.8**	0.5-**1.6**	This study	NA
Fossil taxa												
Tricolporopollenites indeterminatus	Kłodzko, Poland	Pliocene	27-47	35-38	35-40	35-40	1-3	1.0-2.7	0.7-1.5	0.5-1.6	Jahn et al., 1984; Stuchlik et al., 2014	*P. subaequalis*
Tricolporopollenites indeterminatus	Sośnica, Poland	Late Miocene	29-45	39-46	42-49	42-49	1.0-3.0	1.0-2.8	0.5-2.0	0.5-1.5	Stuchlik et al., 2014	*P. subaequalis*
Parrotia sp.	Lavanttal, Austria	Middle Miocene	25-27	34-36	80-85	NO	1.2-1.6	NO	0.7-1.2	NO	Grímsson et al., 2015	*P. persica*
Tricolporopollenites indeterminatus	Legnica, Poland	Middle Miocene	29-30	42-42	60-64	NO	1.0-2.0	NO	0.5-1.0	NO	Stuchlik et al., 2014	*P. persica*
Parrotia sp.	Güvem, Turkey	Early Miocene	33-35	NO	NO	90-95	NO	0.6-1.2	NO	0.5-0.8	Denk et al., 2019	*P. persica*
Tricolporopollenites staresedloensis	Central & Western Paratethys	Late Oligocene/early Miocene	30-32	30-35	45-50	NO	1-1.9	NO	0.5-1.0	NO	Hochuli, 1978	*P. persica*
Parrotiapollenites asper	As Pontes, Spain	Late Oligocene	25-33	NO	NO	85-95	NO	0.7-1.8	NO	0.5-1.0	Casas-Gallego & Barrón, 2021	*P. persica*

Note: All the six quantitative descriptors (compare to Table 1; detailed in Suppl. 1) have been measured when possible. E (µm) = equatorial diameter of pollen. Nlumen = number of lumina per 10 µm^2 of pollen surface, which corresponds to the lumen density in fine. Lll and Wll = length and width of the largest lumen observed in the same 10 µm^2 area. Lsl and Wsl = length and width of the smallest lumen observed in the same 10 µm^2 area. Measurements from original publications or/and based on illustrated fossil pollen.

(i.e. Temperate–oceanic) and n°26 (i.e. Mediterranean–xeric-oceanic) while *P. subaequalis* remains in n°32 (i.e. Temperate–continental) bioclimatic conditions. Unfortunately, the allegedly narrow ecological niche of *P. persica*, is commonly used to infer paleoclimate conditions (temperatures and precipitations) for Eurasian paleoenvironments (Emberger and Sabeti, 1962; Ramezani et al., 2013). But in their publication on the palynoflora from the Lavanttal Basin, Grímsson et al. (2015) referred to several studies focused on *P. persica* providing significant range in the amount of for example annual precipitation, mean annual temperature, elevation, and associated plant species.

Overall, a comparative ecological niche modeling of both extant species is needed in order to put forward a more reliable paleoenvironmental interpretations based on affiliation to either of the extant species. Moreover, because of the restricted distribution of extant *Parrotia* some climatic parameters could be underestimated (e.g. Bruch et al., 2002; Uhl et al., 2007; Thiel et al., 2012).

5. Conclusions

Comparison between pollen grains of *Parrotia persica* (from the Hyrcanian forest of Iran and Azerbaijan) and *P. subaequalis* (from temperate forests of south-eastern China) demonstrates significant morphological differences. The two-species LDA ultimately provides a linear discriminant classifier so dispersed pollen grains can be assigned to either species based on six analyzed descriptors. This distinction can be done using simple light microscopy; *P. subaequalis* is characterized by large and sparse lumina, and *P. persica* is best identified by small and dense lumina. Until now, palaeopalynological studies, affiliated fossil *Parrotia* type pollen automatically as being grains of *P. persica*. The recent discovery of the sibling *P. subaequalis* and now, with our study, the demonstration of its significant difference in pollen morphology when compared to *P. persica* led to re-evaluate the former palaeoenvironmental estimations, especially in Europe where the fossil records between Late Miocene to Pliocene support an affiliation to *P. subaequalis* pollen type. Such observation could suggest a divergence within *Parrotia* and the emergence of the new species, that is now restricted to Eastern Asia.

Declaration of Competing Interest

The authors declare that they have no known competing financial interests or personal relationships that could have appeared to influence the work reported in this paper.

Acknowledgements

We thank Mrs. Xuefeng Yang (杨雪峰) who collected and provided to us the flower of the species *Parrotia subaequalis* from China. We are also grateful to Hossein Akhani who provided photographs of *Parrotia persica* pollen from Iran. Overall, we thank the respective teams from China and Iran. Helpful discussion with Thomas Denk is acknowledged.

We thank reviewers Prof. Gonzalo Jiménez-Moreno and one anonymous reviewer for their work.

This work was supported by a grant from Carl Tryggers Stiftelse (project no. CTS21: 1585).

The following are the supplementary data related to this article.

References

Adroit, B., Malekhosseini, M., Girard, V., Abedi, M., Rajaei, H., Terral, J.-F., Wappler, T., 2018. Changes in pattern of plant-insect interactions on the Persian ironwood (Parrotia persica, Hamamelidaceae) over the last 3 million years. Rev. Palaeobot. Palynol. 258, 22–35. https://doi.org/10.1016/j.revpalbo.2018.06.007.

Adroit, B., Zhuang, X., Wappler, T., Terral, J.-F., Wang, B., 2020. A case of long-term herbivory: specialized feeding trace on Parrotia (Hamamelidaceae) plant species. R. Soc. Open Sci. 7, 14.

Akhani, H., 1998. Plant biodiversity of Golestan National Park, Iran. Stapfia. 53, 1–411.

Akhani, H., Djamali, M., Ghorbanalizadeh, A., Ramezani, E., 2010. Plant biodiversity of Hyrcanian relict forests, N Iran: an overview of the flora, vegetation, palaeoecology and conservation. Pak. J. Bot. 42, 231–258.
Anderson, M.J., 2001. A new method for non-parametric multivariate analysis of variance. Austral Ecol. 26, 32–46. https://doi.org/10.1111/j.1442-9993.2001.01070.pp.x.
Beug, H.-J., 2004. Leitfaden der Pollenbestimmung: für Mitteleuropa und angrenzende Gebiete. Fischer, Stuttgart, pp. 144–250.
Biltekin, D., Popescu, S.-M., Suc, J.-P., Quézel, P., Jiménez-Moreno, G., Yavuz, N., Namık Çağatay, M., 2015. Anatolia: a long-time plant refuge area documented by pollen records over the last 23 million years. Rev. Palaeobot. Palynol. 215, 1–22. https://doi.org/10.1016/j.revpalbo.2014.12.004.
Bińka, K., Nitychoruk, J., Dzierzek, J., 2003. *Parrotia persica* C.A.M. (Persian witch hazel, Persian ironwood) in the Mazovian (Holsteinian) Interglacial of Poland. Grana 42, 227–233. https://doi.org/10.1080/00173130310016220.
Bogle, A.L., Philbrick, C.T., 1980. A generic atlas of hamamelidaceous pollens. Contrib. Gray Herb. Harv. Univ. 29–103.
Bruch, A.A., Fauquette, S., Bertini, A., 2002. Two quantitative approaches for climate reconstructions on Neogene palynofloras - an application on a late Miocene profile from the Velona Basin (Tuscany, Italy). Acta Univ. Carol. - Geol. 46, 27–37.
Cao, Y.-N., Comes, H.P., Sakaguchi, S., Chen, L.-Y., Qiu, Y.-X., 2016. Evolution of East Asia's Arcto-Tertiary relict Euptelea (Eupteleaceae) shaped by Late Neogene vicariance and Quaternary climate change. BMC Evol. Biol. 16, 66. https://doi.org/10.1186/s12862-016-0636-x.
Cruden, R.W., 1976. Intraspecific variation in pollen-ovule ratios and nectar secretion–preliminary evidence of ecotypic adaptation. Ann. Mo. Bot. Gard. 63, 277–289. https://doi.org/10.2307/2395306.
DeChaine, E.G., Martin, A.P., 2006. Using coalescent simulations to test the impact of quaternary climate cycles on divergence in an alpine plant-insect association. Evolution 60, 1004. https://doi.org/10.1554/05-672.1.
Doornik, J.A., Hansen, H., 1994. An omnibus test for univariate and multivariate normality. Oxf. Bull. Econ. Stat. 70, 927–939. https://doi.org/10.1111/j.1468-0084.2008.00537.x.
Emberger, L., Sabeti, H., 1962. Forêts denses intertropicales et forêts caspiennes humides. Nat. Monspel. Bot. 14, 55–61.
Fang, Y., Jin, Y., Deng, M., Yang, Q., Li, B., 1997. Macroscopic and microscopic structure of *Parrotia subaequalis* leaves and its systemic significance (in Chinese). Plant Resour. Environ. 36–42.
Fick, S.E., Hijmans, R.J., 2017. WorldClim 2: new 1km spatial resolution climate surfaces for global land areas. Int. J. Climatol. 37, 4302–4315.
Follieri, M., Magri, D., Sadori, L., 1986. Late Pleistocene Zelkova extinction in central Italy. New Phytol. 103, 269–273.
Frenzel, B., Pecsi, M., Velichko, A.A. (Eds.), 1992. Atlas of Paleoclimates and Paleoenvironments of the Northern Hemisphere. Late Pleistocene–Holocene. Late Pleistocene–Holocene. Geographical Research Institute, Budapest, and Gustav Fischer Verlag, Stuttgart, pp. 61–63.
Fritz, A., Allesch, K., 1999. Pollenmorphologische Bilddokumenta- tion ausgewählter Sippen der ehemals Kätzchenblütigen. Carinthia II 189 (109), 471–490.
Garfì, G., Buord, S., 2012. Relict species and the challenges for conservation: the emblematic case of Zelkova sicula Di Pasquale, Garfì et Quézel and the efforts to save it from extinction. Biodivers. J. 3, 16.
BIF.org (06 June 2022) GBIF Occurrence Download: *Parrotia subaequalis:* https://doi.org/10.15468/dl.gqzx8n
GBIF.org (06 June 2022) GBIF Occurrence Download: *Parrotia persica:* https://doi.org/10.15468/dl.v8wyjp
Grímsson, F., Meller, B., Bouchal, J.M., Zetter, R., 2015. Combined LM and SEM study of the middle Miocene (Sarmatian) palynoflora from the Lavanttal Basin, Austria: part III. Magnoliophyta 1 – Magnoliales to Fabales. Grana 54, 85–128. https://doi.org/10.1080/00173134.2015.1007081.
Halbritter, H., Ulrich, S., Grímsson, F., Weber, M., Zetter, R., Hesse, M., Buchner, R., Svojtka, M., Frosch-Radivo, A., 2018. Palynology: history and systematic aspects. Illustrated Pollen Terminology. Springer, pp. 3–21.
Hammer, Ø., Harper, D.A.T., Ryan, P.D., 2001. PAST: Paleontological statistics software package for education and data analysis. Palaeontol. Electron. 4, 1–9.
Hedhly, A., Hormaza, J.I., Herrero, M., 2005. Influence of genotype-temperature interaction on pollen performance. J. Evol. Biol. 18, 1494–1502. https://doi.org/10.1111/j.1420-9101.2005.00939.x.
Jiménez-Moreno, G., Suc, J.-P., 2007. Middle Miocene latitudinal climatic gradient in Western Europe: evidence from pollen records. Palaeogeogr. Palaeoclimatol. Palaeoecol. 253, 208–225. https://doi.org/10.1016/j.palaeo.2007.03.040 Miocene climate in Europe - patterns and evolution. First synthesis of NECLIME.
Jiménez-Moreno, G., Popescu, S.M., Ivanov, D., Suc, J.P., 2007. Neogene flora, vegetation and climate dynamics in southeastern Europe and the northeastern Mediterranean. In: Williams, M., Haywood, A.M., Gregory, F.J., Schmidt, D.N. (Eds.), Deep-Time Perspect. Clim. Change Marrying Signal Comput. Models Biol. Proxies, pp. 503–516.
Jiménez-Moreno, G., Fauquette, S., Suc, J.-P., 2010. Miocene to Pliocene vegetation reconstruction and climate estimates in the Iberian Peninsula from pollen data. Rev. Palaeobot. Palynol. 162, 403–415. https://doi.org/10.1016/j.revpalbo.2009.08.001.
Kottek, M., Grieser, J., Beck, C., Rudolf, B., Rubel, F., 2006. World Map of the Köppen-Geiger climate classification updated. Meteorol. Z. 15, 259–263. https://doi.org/10.1127/0941-2948/2006/0130.
Kozlowski, G., Frey, D., Fazan, L., Egli, B., Bétrisey, S., Gratzfeld, J., Garfì, G., Pirintsos, S., 2014. The Tertiary relict tree Zelkova abelicea (Ulmaceae): distribution, population structure and conservation status on Crete. Oryx 48, 80–87. https://doi.org/10.1017/S0030605312001275.
Kvaček, Z., 1998. Bílina: a window on Early Miocene marshland environments. Rev. Palaeobot. Palynol. 101, 111–123. https://doi.org/10.1016/S0034-6667(97)00072-9.
Legendre, P., Legendre, L., 2012. Numerical Ecology. 3rd edition. Elsevier, Amsterdam.
Leroy, S.A., Roiron, P., 1996. Latest Pliocene pollen and leaf floras from Bernasso palaeolake (Escandorgue Massif, Hérault, France). Rev. Palaeobot. Palynol. 94, 295–328.
Li, J.-H., Bogle, A.L., Klein, A.S., 1997. Close relationship between Shaniodendron and Parrotia (Hamamelidaceae), evidence from its sequences of nuclear ribosomal DNA. Acta Phytotaxon. Sin. 481–483.
Li, H., Yue, C., Zhang, Y., Shao, S., Yu, L., 2012. Advance of research on *Parrotia subaequalis* (in Chinese). J. Zhejiang For. Sci. Technol. 32, 79–84.
Liu, J., Zhang, G.-F., Li, X., 2021. Structural diversity and conservation implications of *Parrotia subaequalis* (Hamamelidaceae), a rare and endangered tree species in China. Nat. Conserv. 44, 99–115. https://doi.org/10.3897/natureconservation.44.69404.
Manchester, S.R., Chen, Z.-D., Lu, A.-M., Uemura, K., 2009. Eastern Asian endemic seed plant genera and their paleogeographic history throughout the Northern Hemisphere. J. Syst. Evol. 47, 1–42. https://doi.org/10.1111/j.1759-6831.2009.00001.x.
Marquer, L., Gaillard, M.-J., Sugita, S., Trondman, A.-K., Mazier, F., Nielsen, A.B., Fyfe, R., Odgaard, B.V., Alenius, T.B., Birks, H.J., Bjune, A.E., Christiansen, J., Dodson, J., Edwards, K.J., Giesecke, T., Herzschuh, U., Kangur, M., Lorenz, S., Poska, A., Schult, M., Seppä, H., 2014. Holocene changes in vegetation composition in northern Europe: why quantitative pollen-based vegetation reconstructions matter. Quat. Sci. Rev. 90, 199–216. https://doi.org/10.1016/j.quascirev.2014.02.013.
Martin, A.C., Harvey, W.J., 2017. The Global Pollen Project: a new tool for pollen identification and the dissemination of physical reference collections. Methods Ecol. Evol. 8, 892–897. https://doi.org/10.1111/2041-210X.12752.
Milne, R.I., 2006. Northern hemisphere plant disjunctions: a window on tertiary land bridges and climate change? Ann. Bot. 98, 465–472. https://doi.org/10.1093/aob/mcl148.
Nagalingum, N.S., Marshall, C.R., Quental, T.B., Rai, H.S., Little, D.P., Mathews, S., 2011. Recent synchronous radiation of a living fossil. Science 334, 796–799. https://doi.org/10.1126/science.1209926.
Nakagawa, T., Garfì, G., Reille, M., Verlaque, R., 1998. Pollen morphology of Zelkova sicula (Ulmaceae), a recently discovered relic species of the European Tertiary flora: description, chromosomal relevance, and palaeobotanical significance. Rev. Palaeobot. Palynol. 100, 27–37. https://doi.org/10.1016/S0034-6667(97)00062-6.
Naud, G., Suc, J.P., 1975. Contribution à l'étude paléofloristique des Coisons (Ardèche): premières analyses polliniques dans les alluvions sous-basaltiques et interbasaltiques de Mirabel (Miocène supérieur). Bull. Soc. Géol. Fr. ser. 7, 18 5, 820–827.
Olson, D.M., Dinerstein, E., Wikramanayake, E.D., Burgess, N.D., Powell, G.V.N., Underwood, E.C., D'amico, J.A., Itoua, I., Strand, H.E., Morrison, J.C., Loucks, C.J., Allnutt, T.F., Ricketts, T.H., Kura, Y., Lamoreux, J.F., Wettengel, W.W., Hedao, P., Kassem, K.R., 2001. Terrestrial ecoregions of the world: a new map of life on earth: a new global map of terrestrial ecoregions provides an innovative tool for conserving biodiversity. BioScience 51, 933–938. https://doi.org/10.1641/0006-3568(2001)051[0933:TEOTWA]2.0.CO;2.
Paridari, I.C., Jalali, S.G., Sattarian, A., Zarafshar, M., Sonboli, A., 2012. Pollen grain morphology of *Parrotia persica* (Hamamelidaceae) an endemic species from the Hyrcanian forest. Ann. Biol. Res. 3 (2), 1157–1160.
Peel, M.C., Finlayson, B.L., McMahon, T.A., 2007. Updated world map of the Köppen-Geiger climate classification. Hydrol. Earth Syst. Sci. 11, 1633–1644. https://doi.org/10.5194/hess-11-1633-2007.
Popescu, S.-M., Suc, J.-P., Fauquette, S., Bessedik, M., Jiménez-Moreno, G., Robin, C., Labrousse, L., 2021. Mangrove distribution and diversity during three Cenozoic thermal maxima in the Northern Hemisphere (pollen records from the Arctic–North Atlantic–Mediterranean regions). J. Biogeogr. 48, 2771–2784. https://doi.org/10.1111/jbi.14238.
Punt, W., Hoen, P.P., Blackmore, S., Nilsson, S., Le Thomas, A., 2007. Glossary of pollen and spore terminology. Rev. Palaeobot. Palynol. 143, 1–81. https://doi.org/10.1016/j.revpalbo.2006.06.008.
Qian, H., Ricklefs, R.E., 2000. Large-scale processes and the Asian bias in species diversity of temperate plants. Nature 407, 180–182. https://doi.org/10.1038/35025052.
Ramezani, E., Marvie Mohadjer, M.R., Knapp, H.-D., Theuerkauf, M., Manthey, M., Joosten, H., 2013. Pollen–vegetation relationships in the central Caspian (Hyrcanian) forests of northern Iran. Rev. Palaeobot. Palynol. 189, 38–49. https://doi.org/10.1016/j.revpalbo.2012.10.004.
Rivas-Martinez, S., Rivas-Saenz, S., Penas, A., 2011. Worldwide Bioclimatic Classification System. Global Geobotany 1, 1–634.
Reille, M., Beaulieu, J.-L.D., Svobodova, H., Andrieu-Ponel, V., Goeury, C., 2000. Pollen analytical biostratigraphy of the last five climatic cycles from a long continental sequence from the Velay region (Massif Central, France). J. Quat. Sci. 15, 665–685. https://doi.org/10.1002/1099-1417(200010)15:7<665::AID-JQS560>3.0.CO;2-G.
Rencher, A.C., Christensen, W.F., 2012. Methods of Multivariate Analysis. 3rd edition. Wiley.
Rubel, F., Brugger, K., Haslinger, K., Auer, I., 2017. The climate of the European Alps: shift of very high resolution Köppen-Geiger climate zones 1800–2100. Meteorol. Z. 115–125. https://doi.org/10.1127/metz/2016/0816.
Sagheb-Talebi, K., Sajedi, T., Pourhashemi, M., 2014. Forests of Iran: A Treasure from the Past, A Hope for the Future. Plant and Vegetation 10. Springer, Dordrecht.
Sattarian, A., Reza Akbarian, M., Zarafshar, M., Bruschi, P., Fayyaz, P., 2011. Phenotypic variation and leaf fluctuating asymmetry in natural populations of Parrotia persica (Hamamelidaceae), an endemic species from the Hyrcanian forest (Iran). Acta Bot. Mex. 97, 65–81.
Sefidi, K., Marvie Mohadjer, M.R., Etemad, V., Copenheaver, C.A., 2011. Stand characteristics and distribution of a relict population of Persian ironwood (Parrotia persica C.A. Meyer) in northern Iran. Flora – Morphol. Distrib. Funct. Ecol. Plants 206, 418–422. https://doi.org/10.1016/j.flora.2010.11.005.

Shatilova, I., Mchedlishvili, N., Rukhadze, L., Kvavadze, E., 2011. The History of the Flora and Vegetation of Georgia. Georgian National Museum, Institute of Paleobiology, Tbilisi.

Sokal, R.R., Rohlf, F.J., 1995. Biometry the Principles and Practice of Statistics in Biological Research. Third edition. W.H. Freeman and Co, New York.

Stachurska, A., Sadowska, A., Dyjor, S., 1973. Neogene flora at Sosnica near Wroclaw in the light of geological, and palynological investigations. Acta Palaeobot. 14, 147–176.

Suan, G., Popescu, S.-M., Suc, J.-P., Schnyder, J., Fauquette, S., Baudin, F., Yoon, D., Piepjohn, K., Sobolev, N.N., Labrousse, L., 2017. Subtropical climate conditions and mangrove growth in Arctic Siberia during the early Eocene. Geology 45, 539–542. https://doi.org/10.1130/G38547.1.

Suc, J., Popescu, S., 2005. Pollen records and climatic cycles in the North Mediterranean region since 2.7 Ma. Spec. Publ.-Geol. Soc. Lond. 247, 147.

Suc, J.-P., Fauquette, S., Popescu, S.-M., Robin, C., 2020. Subtropical mangrove and evergreen forest reveal Paleogene terrestrial climate and physiography at the North Pole. Palaeogeogr. Palaeoclimatol. Palaeoecol. 551, 109755. https://doi.org/10.1016/j.palaeo.2020.109755.

Thiel, C., Klotz, S., Uhl, D., 2012. Palaeoclimate estimates for selected leaf floras from the late Pliocene (Reuverian) of Central Europe based on different palaeobotanical techniques. Turk. J. Earth Sci. 21, 263–287.

Uhl, D., Klotz, S., Traiser, C., Thiel, C., Utescher, T., Kowalski, E., Dilcher, D.L., 2007. Cenozoic paleotemperatures and leaf physiognomy — a European perspective. Palaeogeogr. Palaeoclimatol. Palaeoecol. 248, 24–31. https://doi.org/10.1016/j.palaeo.2006.11.005.

UNESCO, 2019. 43rd Session of the World Heritage Committee. Convetion Prot. World Cult. Nat. Herit.

Yosefzadeh, H., Tabari, M., Akbarinia, M., Akbarian, M.R., Bussotti, F., 2010. Morphological plasticity of *Parrotia persica* leaves in eastern Hyrcanian forests (Iran) is related to altitude. Nord. J. Bot. 28, 344–349. https://doi.org/10.1111/j.1756-1051.2009.00451.x.

Zhang, Y.-Y., Shi, E., Yang, Z.-P., Geng, Q.-F., Qiu, Y.-X., Wang, Z.-S., 2018a. Development and application of genomic resources in an endangered palaeoendemic tree, *Parrotia subaequalis* (Hamamelidaceae) from eastern China. Front. Plant Sci. 9, 246. https://doi.org/10.3389/fpls.2018.00246.

Zhang, L., Yang, J., Huang, Y., Jia, Z., Fang, Y., 2018b. Leaf venation variation and phenotypic plasticity in response to environmental heterogeneity in *Parrotia subaequalis* (H. T. Chang) R. M. Hao et H. T. Wei, an endemic and endangered tree species from China. Forests 9, 247. https://doi.org/10.3390/f9050247.

Zhi-chen, S., Wei-ming, W., Fei, H., 2004. Fossil pollen records of extant angiosperms in China. Bot. Rev. 70, 425–458.